INL/CON-23-74904-Revision-0

Understanding grain boundary segregation under irradiation: A mesoscale modeling study

October 2023

Sourabh Bhagwan Kadambi, Jia-Hong Ke, Boopathy Kombaiah, Mukesh Bachhav

INL/CON-23-74904-Revision-0

Understanding grain boundary segregation under irradiation: A mesoscale modeling study

Sourabh Bhagwan Kadambi, Jia-Hong Ke, Boopathy Kombaiah, Mukesh Bachhav

October 2023

Idaho National Laboratory
Idaho Falls, Idaho 83415

http://www.inl.gov

Prepared for the
U.S. Department of Energy
Under DOE Idaho Operations Office
Contract DE-AC07-05ID14517

Understanding grain boundary segregation under irradiation: A mesoscale modeling study

Sourabh B. Kadambi

Computational Mechanics & Materials Department
Nuclear Science & Technology
Idaho National Laboratory

Radiation-induced segregation in steels

Cr enrichment in Fe-6Cr (at.%) at low T [1]

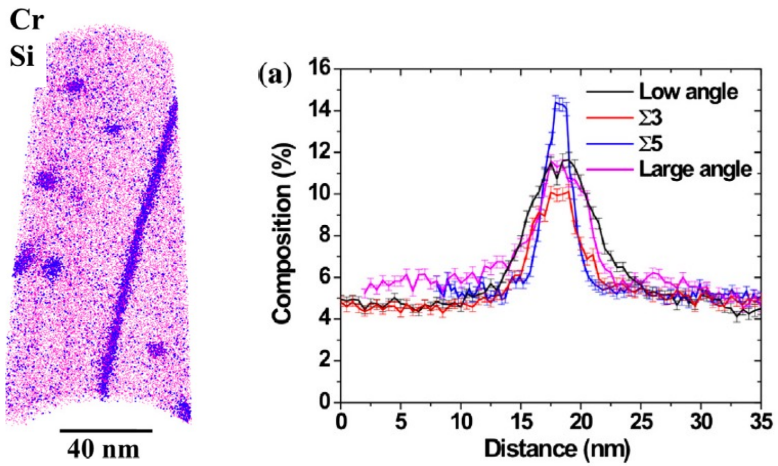

APT profile of neutron irradiated Fe-6at.% Cr (1.82 dpa, 290 C)

RIS in additively manufactured 316L SS [2]

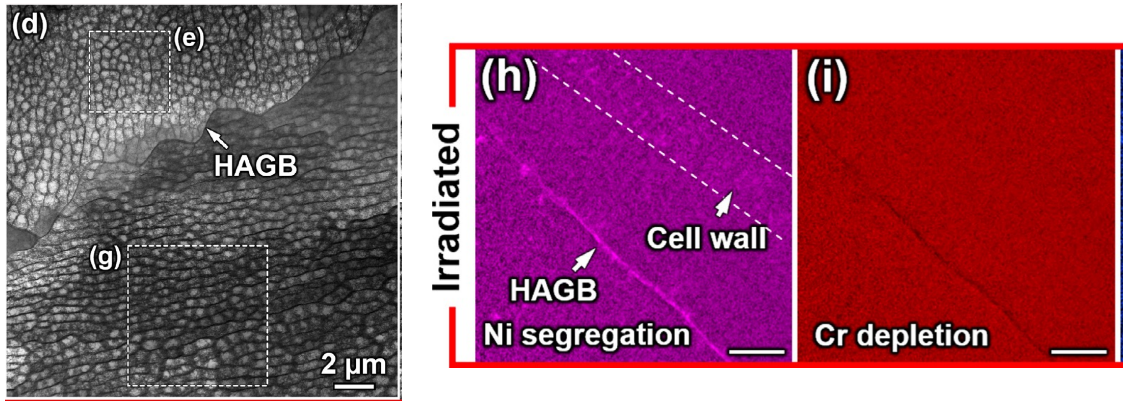

TEM/ HAADF STEM images of 3.5 MeV Fe^{++} irradiated AM 316LN SS
(3×10^{-3} dpa/s, 450 C)

- Complex dependence on temperature, irradiation conditions and material/ microstructural features
- *Required modeling capability: multicomponent kinetics, non-ideal GB sink, RIS at dislocation cell walls*

[1] Bachhav et al., J. Nucl. Mater. 453 (2014)334 – 339
[2] Z. Shang., Journal of Nuclear Materials 546 (2021) 152745

Radiation induced segregation (RIS): theory

Atom-vacancy exchange mechanism

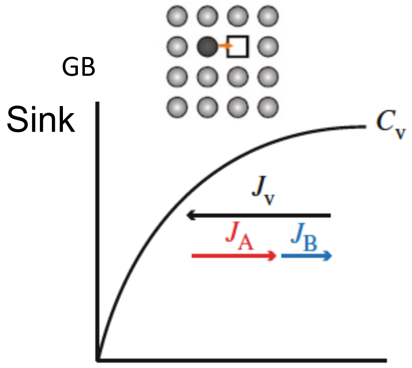

Self-interstitial dumbbell mechanism

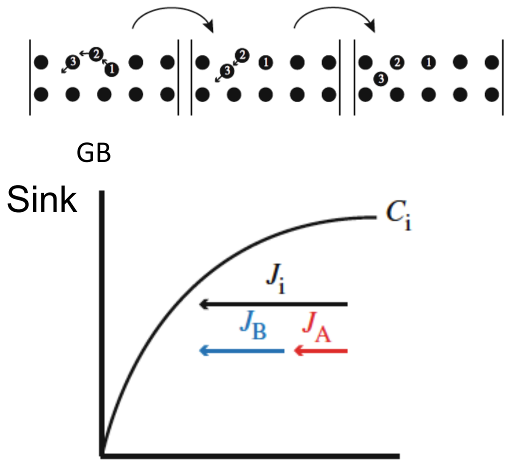

Atomic redistribution

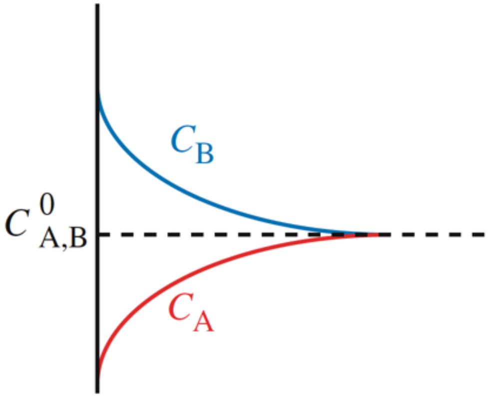

Enrichment/ depletion of atoms due to difference in diffusivities

[1] Was, G. S. Fundamentals of Radiation Materials Science, Springer (2016)
[2] Ardell and Bellon, Curr. Opin. Solid State Mater Sci. 20(3) (2016) 115

Radiation induced segregation (RIS): theory

Fluxes for atoms A, B, C…

$$J_A^V = -L_{AA}^V \nabla(\mu_\mathrm{A} - \mu_V) - L_{AB}^V \nabla(\mu_B - \mu_V) - \cdots$$

$$J_A^I = -L_{AA}^I \nabla(\mu_A + \mu_I) - L_{AB}^I \nabla(\mu_B + \mu_I) - \cdots$$

$$J_A = J_A^V + J_A^I$$

$$J_A + J_B + J_C = 0$$

Total fluxes (reduced form B, C…)

$$J_B = -\tilde{L}_{BB} \nabla \tilde{\mu}_B - \tilde{L}_{BC} \nabla \tilde{\mu}_C \ldots - L_{BV} \nabla \mu_V - L_{BI} \nabla \mu_I$$ (atoms)

$$J_\nu = -\tilde{L}_{\nu B} \nabla \tilde{\mu}_B - \tilde{L}_{\nu C} \nabla \tilde{\mu}_C \ldots - L_{\nu\nu} \nabla \mu_\nu$$ (defects)

$$J_V = J_I$$

[1] Wolfer, W.G., J. Nucl. Mat., 114 (1983) 292–304
[2] Aagesen et al., Comp. Mat. Sci. 161 (2019) 35–45

Phase-field modeling of RIS

Chemical potential-based diffusion, rate theory

(atoms) $$\chi_B \frac{\partial \tilde{\mu}_B}{\partial t} + \chi_{BC} \frac{\partial \tilde{\mu}_C}{\partial t} + \cdots = -\nabla . J_B$$

(defects) $$\chi_{vv} \frac{\partial \mu_v}{\partial t} = -\nabla . J_v + \underbrace{\dot{P}_v}_{\text{Production}} - \underbrace{\dot{R}_{VI} c_V c_I}_{\text{Recombination}} - \underbrace{\dot{S}_v(\eta) c_v}_{\text{Sink}}$$

- Full thermodynamic & kinetic coupling
- Model alloys: FCC FeCrNi, BCC FeCr
- MOOSE: open-source, finite element, C++

MOOSE

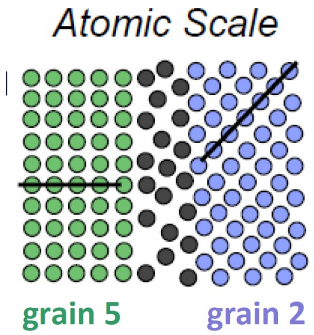

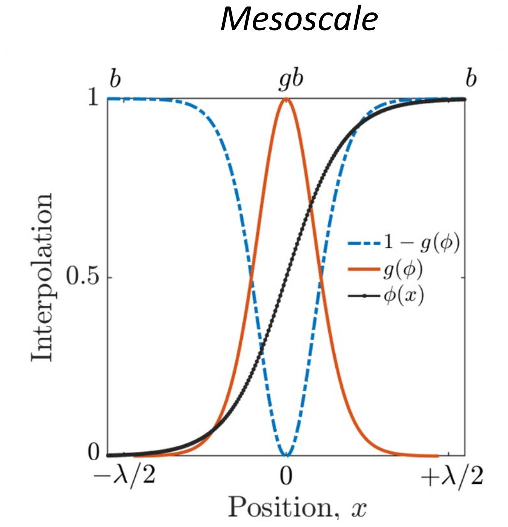

[1] Kadambi, S. B., Schwen, D., Zhang, Y. & He, L.. Phase–field Modeling of Radiation Induced Segregation in Multicomponent Alloys: Kinetic Monte Carlo and CALPHAD Informed Simulations. *Under Preparation*.
[2] MOOSE workshop, PhaseField, INL

Application to additively manufactured FCC Fe-Cr-Ni

Sourabh Kadambi, Lingfeng He[1], Andrea Jokisaari

[1] North Carolina State University

Funded by AMMT and INL's LDRD program

Model parameterization for FCC FeCrNi

- Vacancy transport: CALPHAD-type assessment from experimental tracer diffusivity data [1]
- SIA diffusivity (difficult to compute): **(i) assumed equal** [2], (ii) binding energies from atomistic calculation

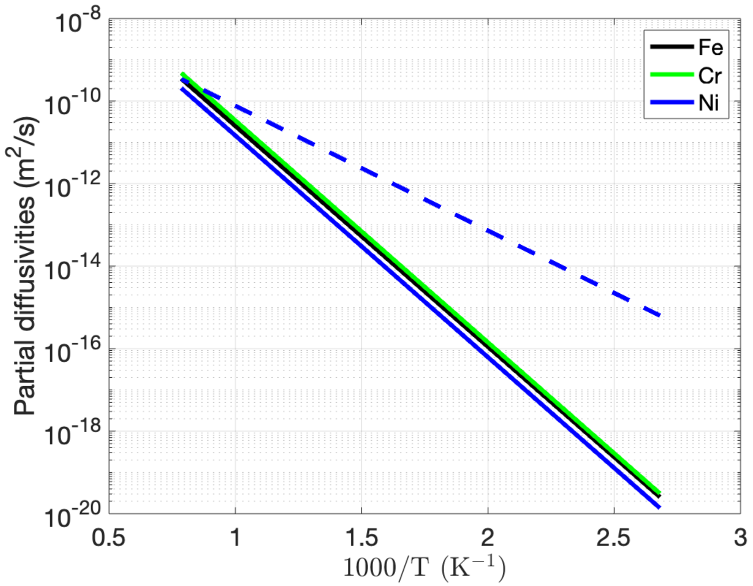

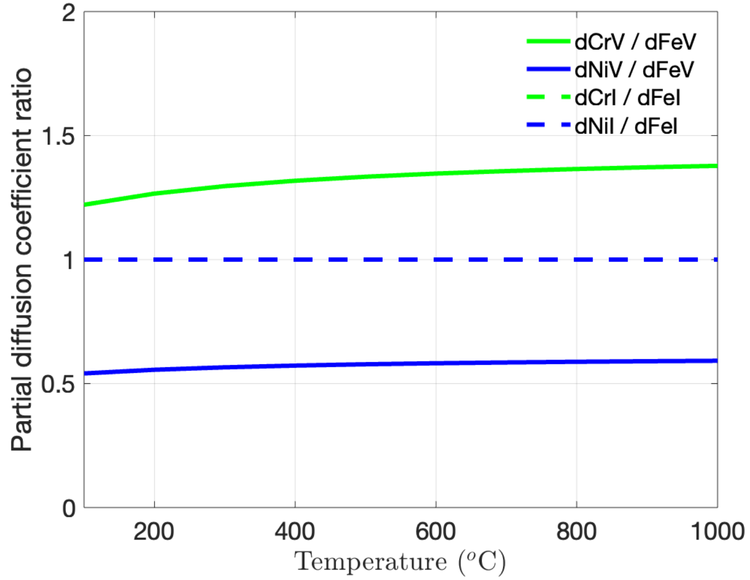

[1] Yang et al., J. Nucl. Mater. 473 (2016) 35 – 53
[2] Allen et al., J. Nucl. Mater. 255 (1998)44 – 58 (MIK model)

Model parameterization for FCC FeCrNi

- Vacancy transport: CALPHAD-type assessment from experimental tracer diffusivity data [1]
- SIA diffusivity (difficult to compute): (i) assumed equal, **(ii) binding energies from atomistic calculation**

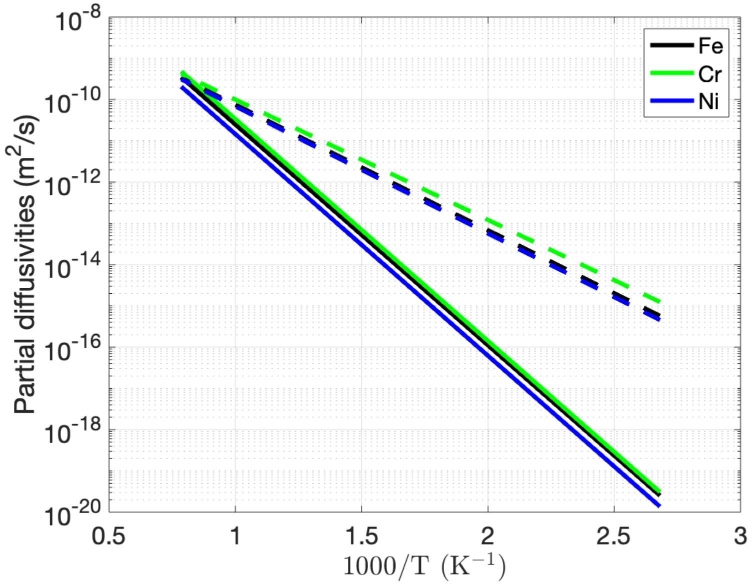

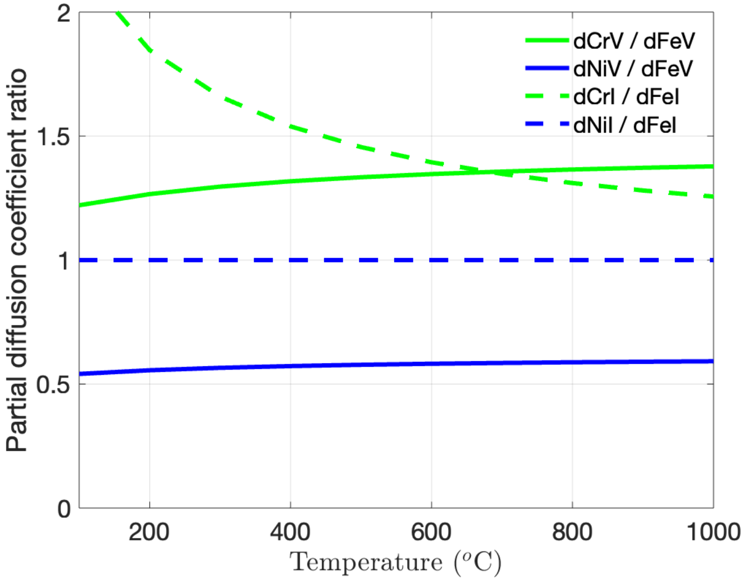

[1] Yang et al., J. Nucl. Mater. 473 (2016) 35 – 53
[2] Allen et al., J. Nucl. Mater. 255 (1998)44 – 58 (MIK model)

Results: effect of grain boundary sink strength

RIS in Fe-17Cr-12Ni (at.%)

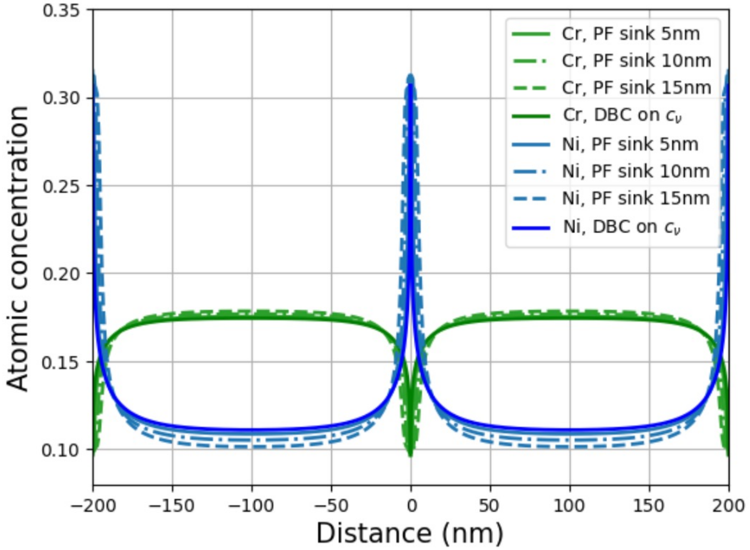

RIS vs. radiation damage

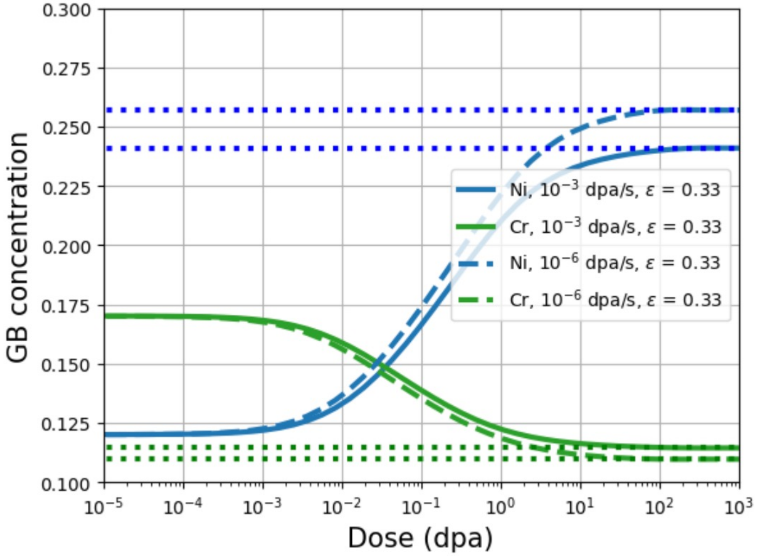

Dose rate dependence

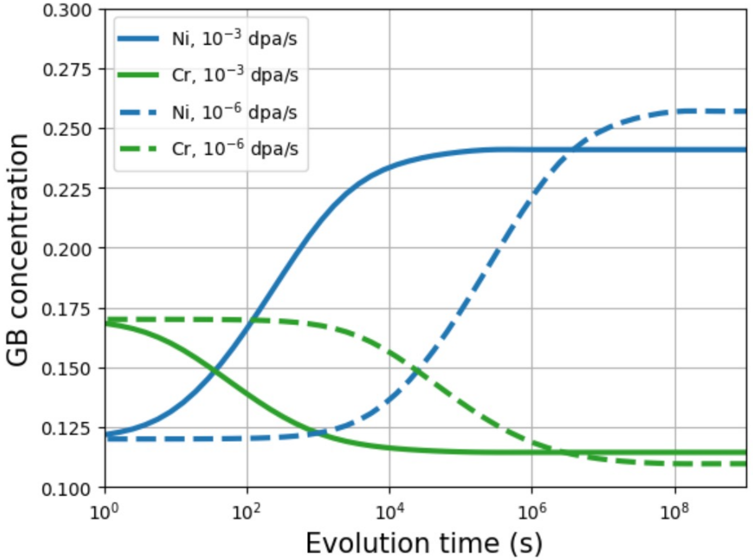

RIS from Dirichlet BC/ sharp interface is compared against sink absorption rate across diffuse phase-field sink for ideal HAGB

Results: effect of grain boundary sink strength

Grain size dependence

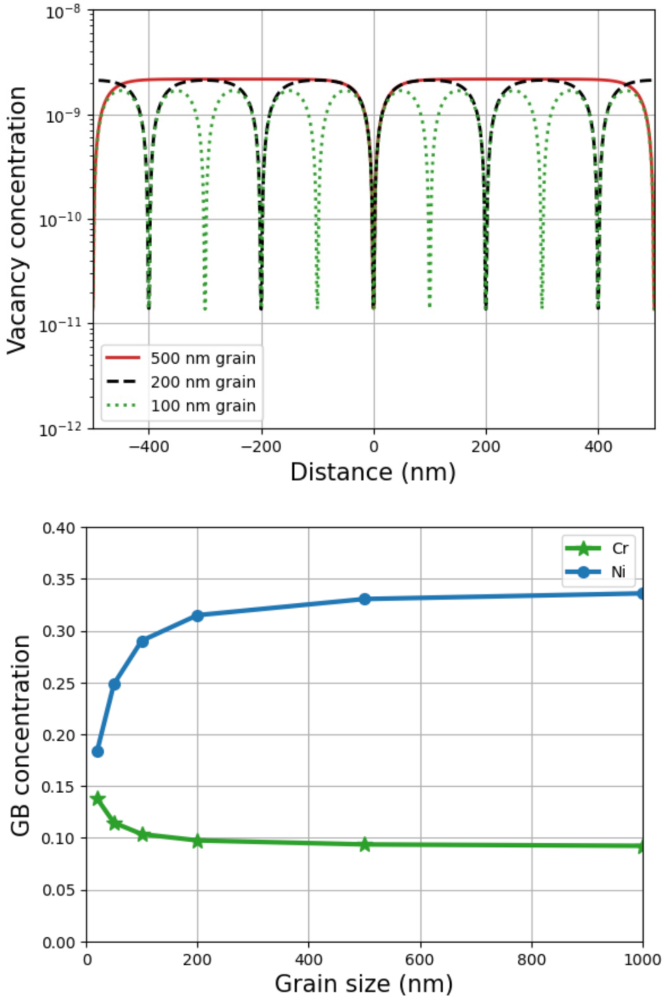

GB structure dependence [1]

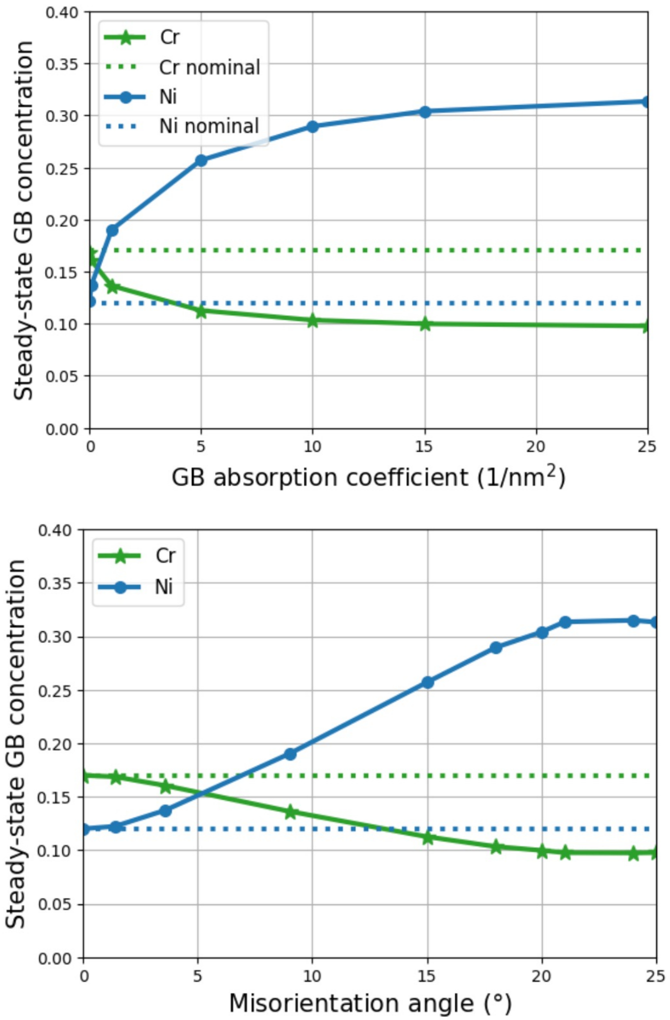

Dimensional sink strength of ideal GB is above 25 nm^{-2} for misorientation above 21°

[1] L. D. Xia et al., Nuclear Engineering and Technology 52 (2020) 148 – 154

RIS in AM microstructure: dislocation cell walls

Diffuse interface description

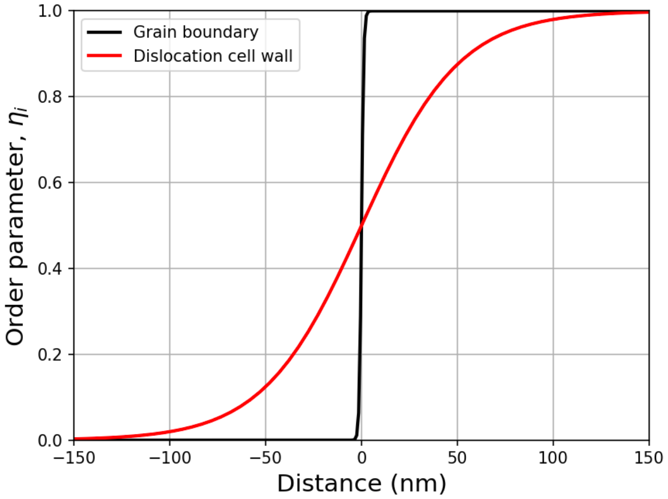

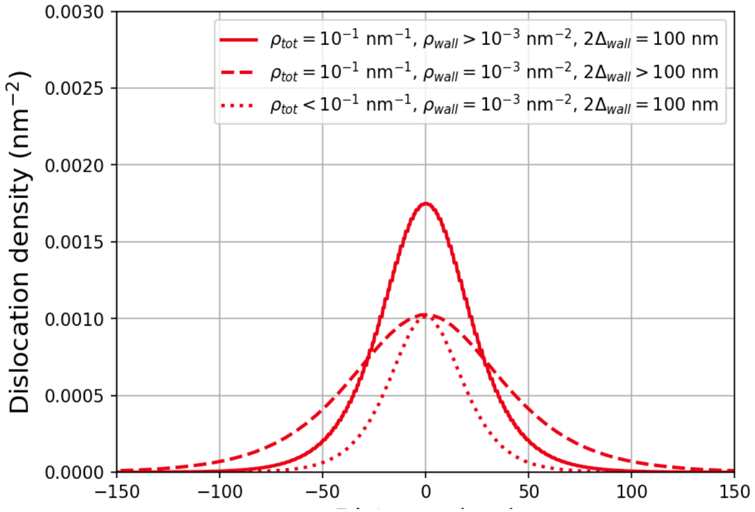

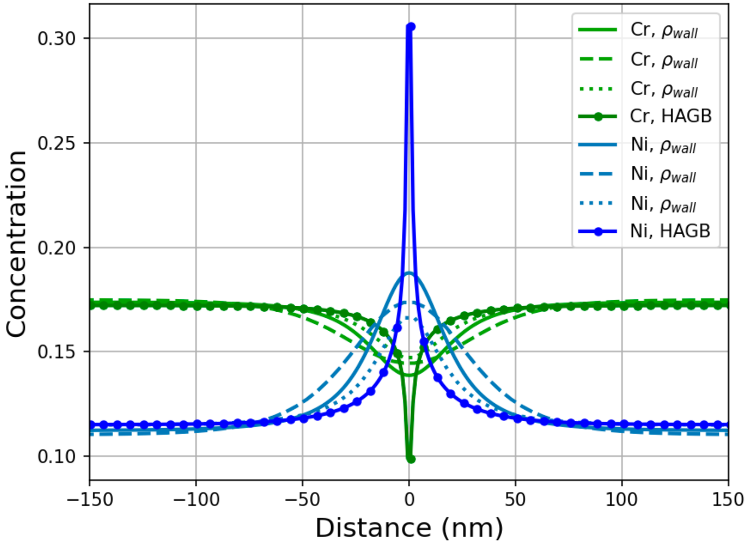

Sink absorption rate are a function of dislocation density (time/ damage dependent)

Dimensional sink strength of 0.025 nm^{-2} was used for dislocation density of 10^{-3} nm^{-2}

RIS in AM microstructure: 2D simulation

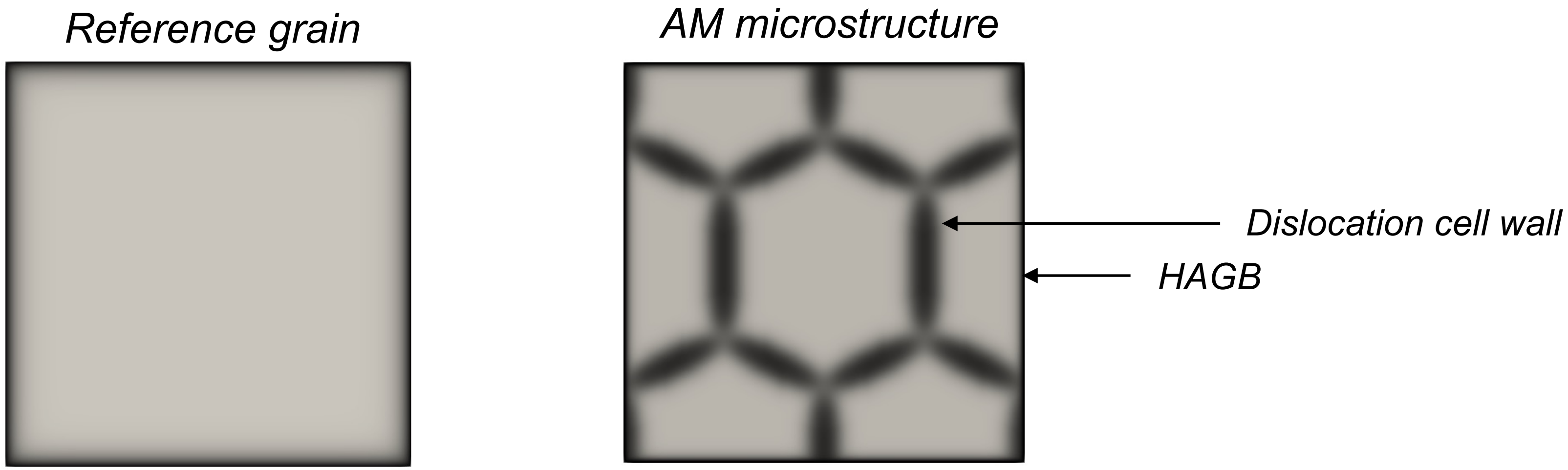

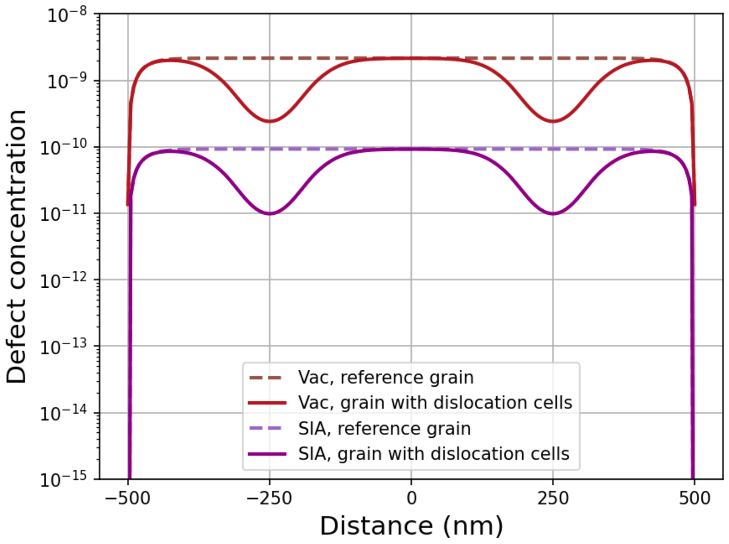

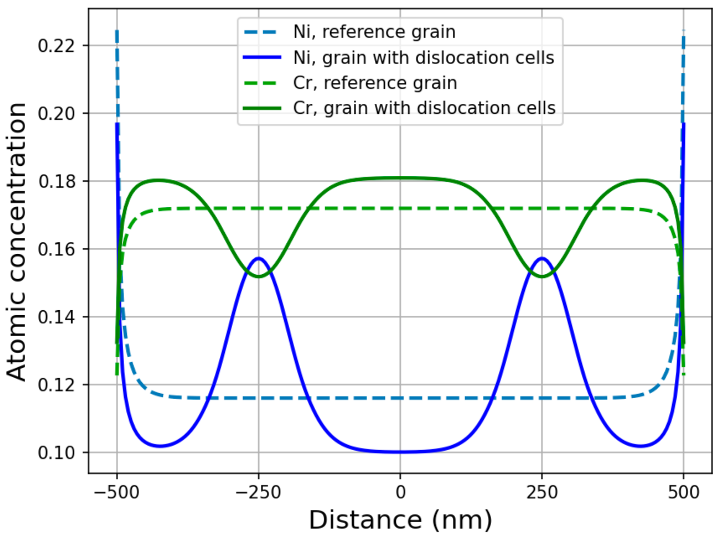

- Lower RIS at HAGB in AM grain due to network dislocations acting as additional sinks
- Demonstrates effect of microstructural features on fluxes reaching GB

RIS in AM microstructure: 2D simulation

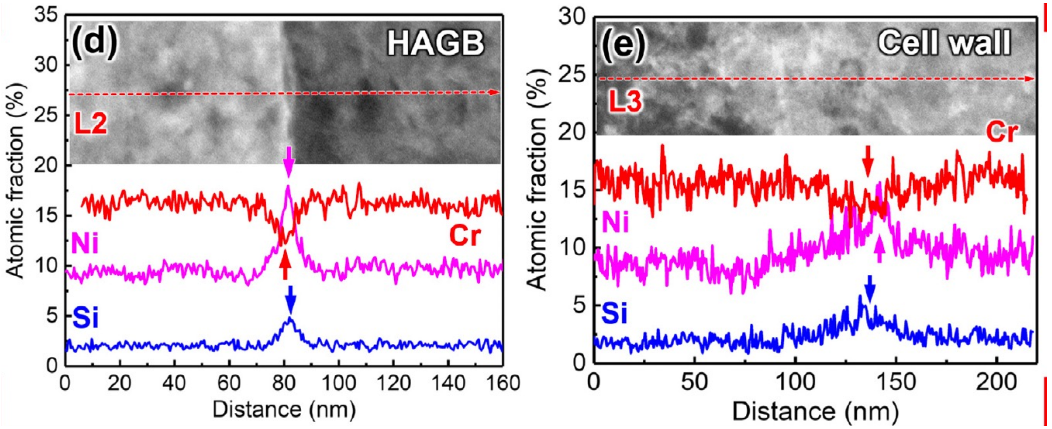

Z. Shang, C. Fan, J. Ding et al.,Journal of Nuclear Materials 546 (2021) 152745

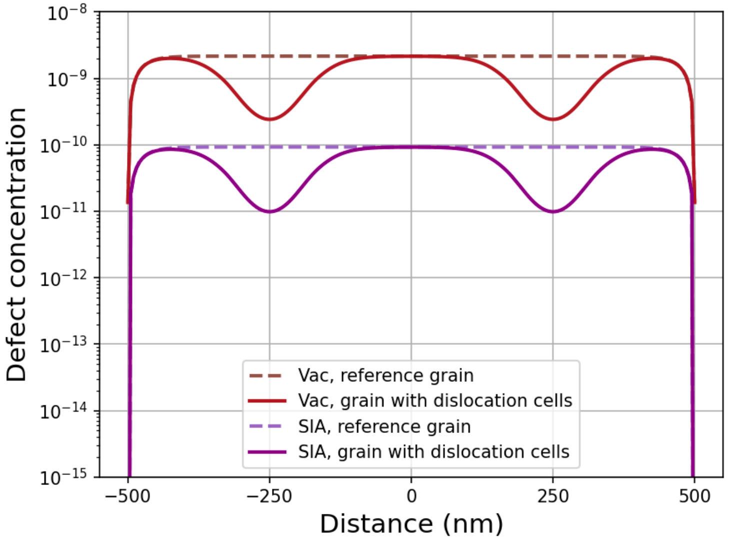

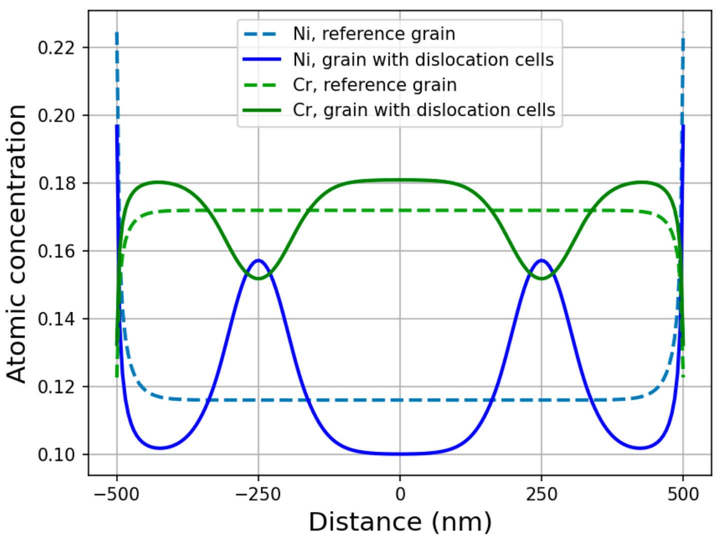

- Lower RIS at HAGB in AM grain due to network dislocations acting as additional sinks
- Demonstrates effect of microstructural features on fluxes reaching GB

Application to BCC Fe-Cr alloy

Sourabh Kadambi, Jia-Hong Ke, Boopathy Kombaiah, Mukesh Bachhav

Funded by INL's LDRD program

Model parameterization for BCC FeCr

DFT data [1] is provided as input to Kinetic Cluster Expansion (KineCluE) [2] model to compute dilute limit Onsager transport coefficients

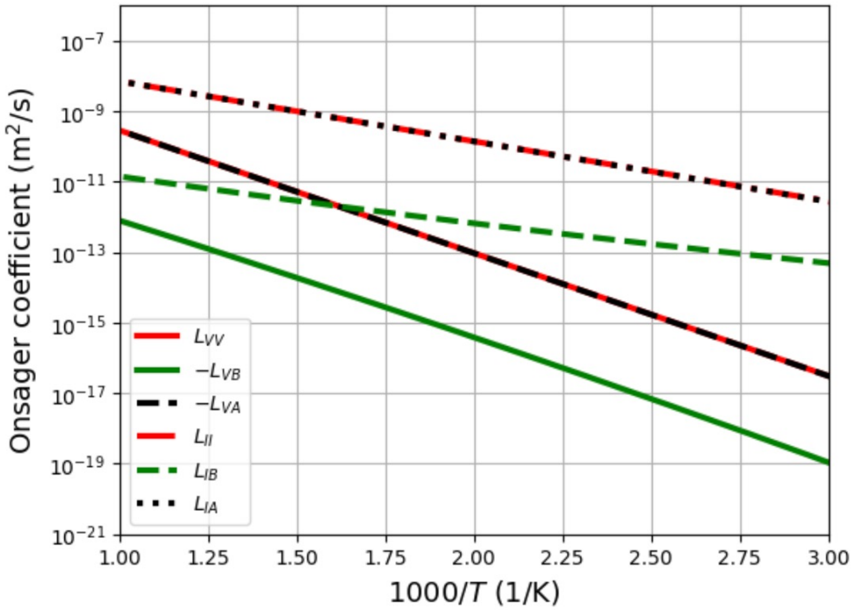

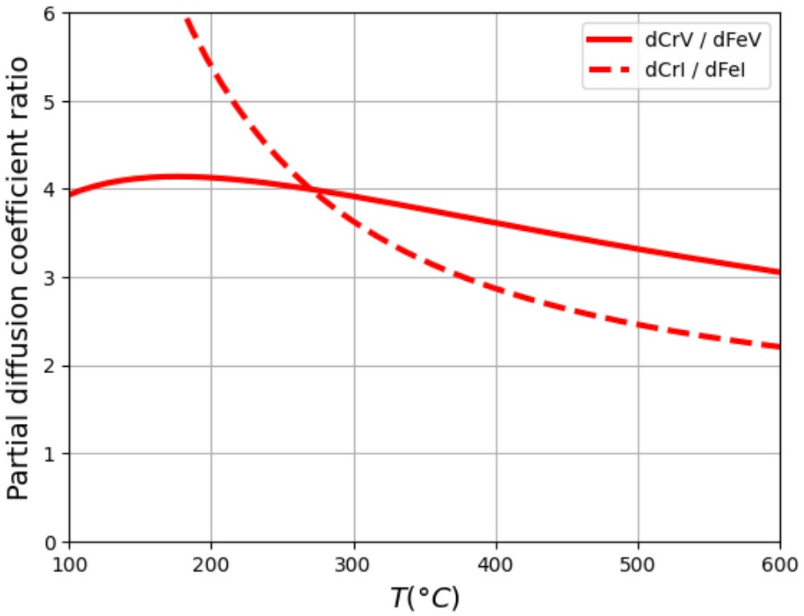

[1] T. Schuler, et al., Computational Materials Science 172 (2020) 109191
[2] L. Messina, et al., Physical Review B 90, 104203 (2014)

RIS in BCC FeCr: cross-over in segregation

Phase-field prediction using KineClUE model for Fe-0.1Cr (at.%)

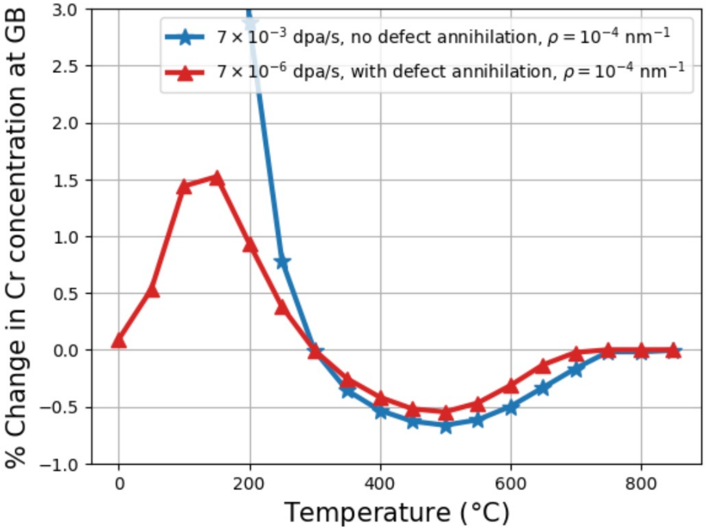

Need to extend capability to Fe-9Cr and determine physically relevant recombination rates

Fe-9Cr (at.%), Wharry-Was (2014)

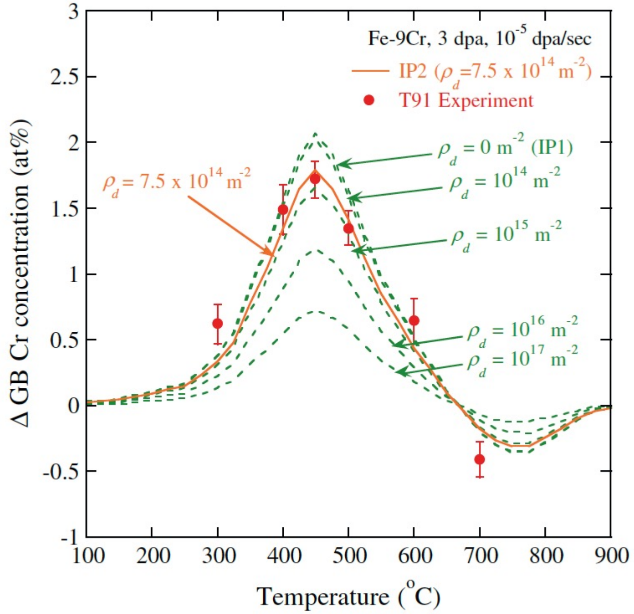

Described bell-shape as resulting from temperature dependent diffusivity, recombination effects

[1] J.P. Wharry, G.S. Was, Acta Materialia 65 (2014) 42–55
[2] L. D. Xia et al. , Nuclear Engineering and Technology 52 (2020) 148 – 154

Spinodal decomposition under irradiation

Nominal concentration < critical spinodal

Nominal concentration > critical spinodal

Thermal, bulk

Irradiation, GB sink

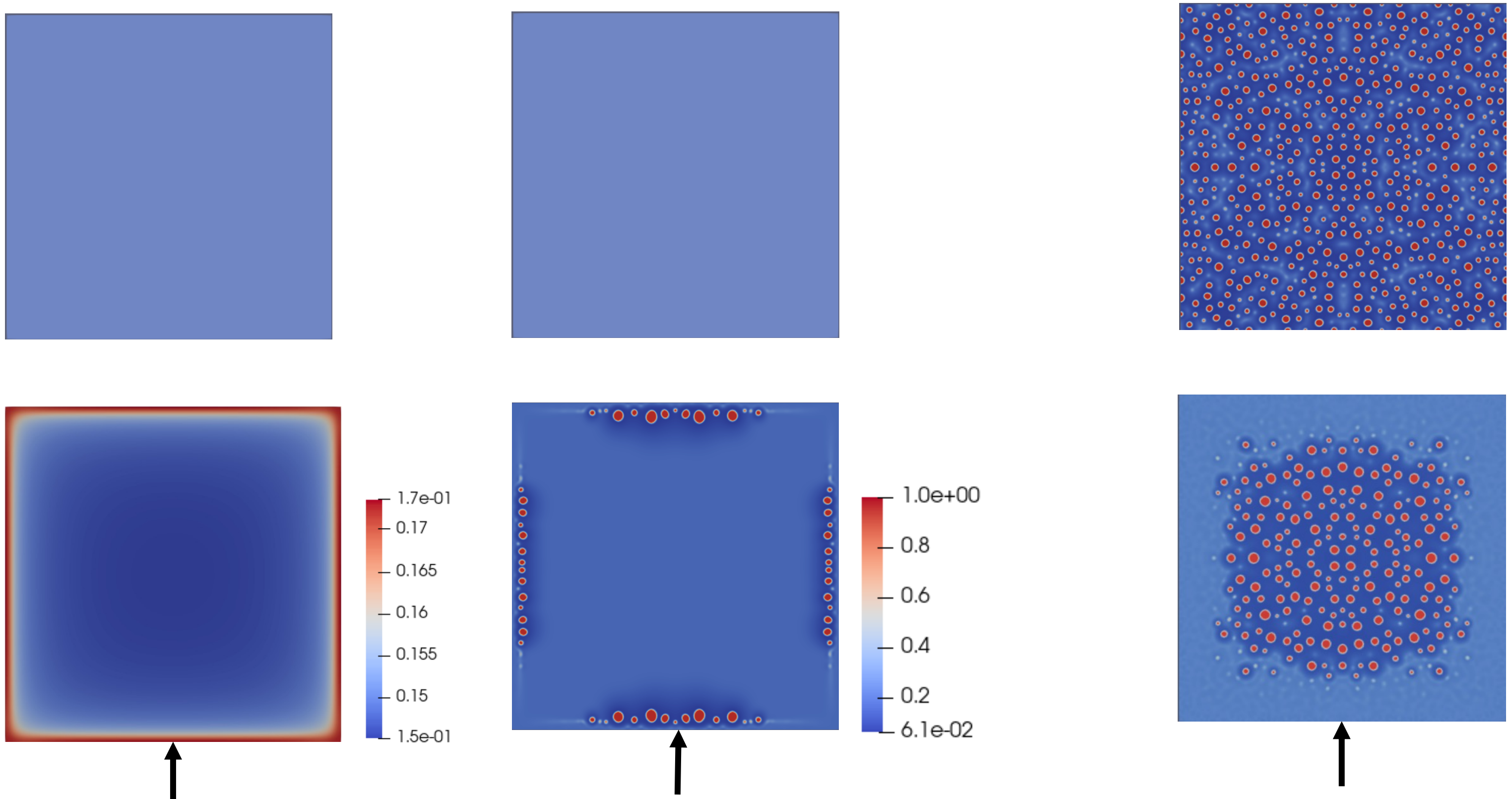

RIS near GB

Spinodal decomposition due to RIS

Denuded zone

- Accelerated kinetics within grain due to higher point defect concentrations under irradiation
- Slow kinetics near GB due to GB sink effect reducing point defect concentration

[1] J.P. Wharry, G.S. Was, Acta Materialia 65 (2014) 42–55
[2] L. D. Xia et al. , Nuclear Engineering and Technology 52 (2020) 148 – 154

Nucleation under irradiation

(Red) Equilibrium $\alpha - \alpha'$ phase boundary using Calphad free energy

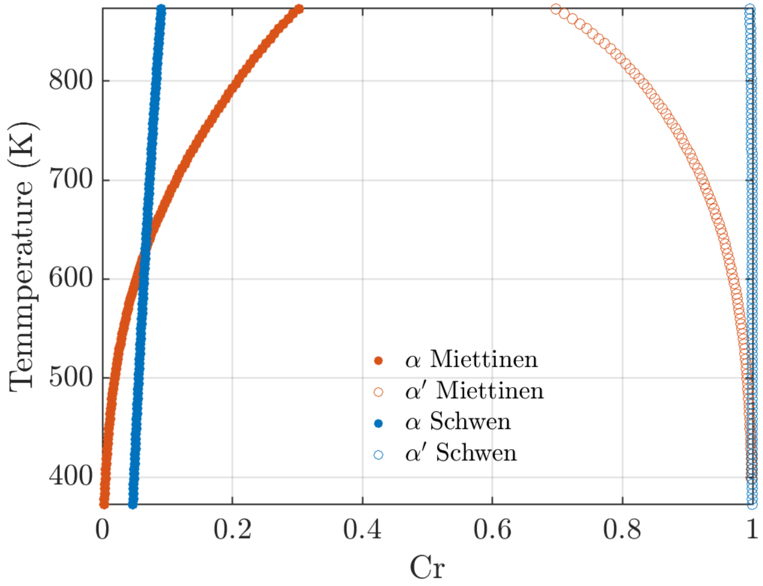

Critical nucleation barrier:

$$\Delta G^*_{nucl} = f^{\alpha'}_{eq} - f \; - \left(c^{\alpha'}_{eq} - c\;\right)\tilde{\mu}$$

Classical nucleation rate:

$$\tilde{J}^* = \tilde{k}_1 \left(\frac{D_{Cr}}{{\Delta G^*_{nucl}}^{n}}\right) \exp\left(-\frac{k_2}{\Delta G^*_{nucl}}\right)$$

Nominal Cr concentration > solvus

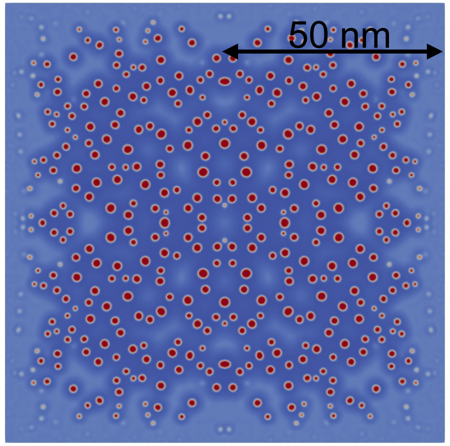

- High nucleation probability and kinetics (Cr mobility) due to excess point defect concentration
- Ballistic mixing is expected to alter $\alpha - \alpha'$ phase boundary/ stability

Nominal Cr concentration = solvus

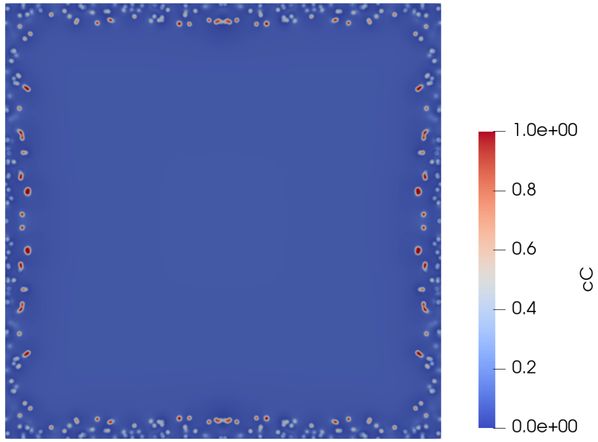

- RIS at GB increases Cr concentration above solubility limit
- Slow nucleation rate and growth kinetics due to low point defect concentration near GB

[1] Miettinen, Calphad 15(4) (1991) 317—425

[2] D. Schwen, et al., Journal of Nucl. Mater. 439 (2013) 180—184

Nucleation under irradiation

Nominal Cr concentration > solvus

Nominal Cr concentration = solvus

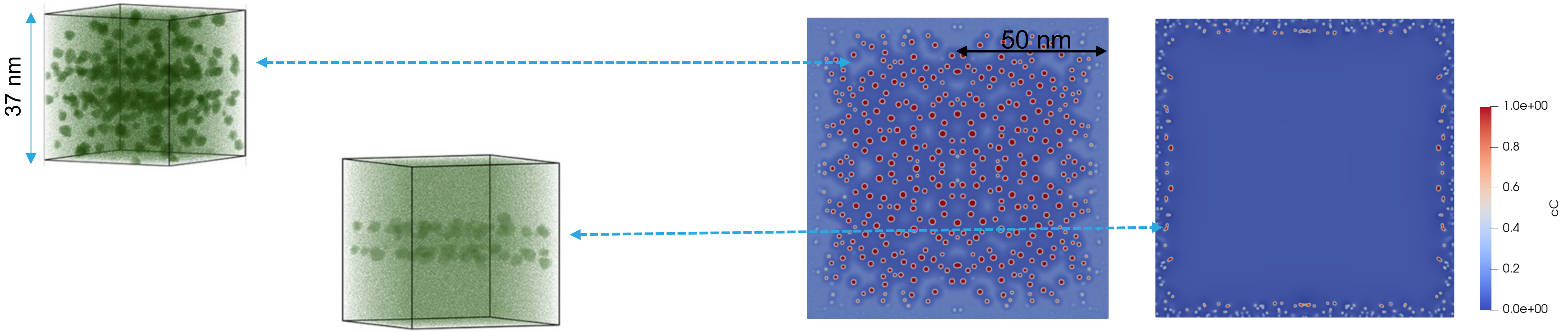

Phase-field predictions are consistent with Atomistic KMC simulations at 290 C [1,2]

- High nucleation probability and kinetics (Cr mobility) due to excess point defect concentration
- Ballistic mixing is expected to alter $\alpha - \alpha'$ phase boundary/ stability

- RIS at GB increases Cr concentration above solubility limit
- Slow nucleation rate and growth kinetics due to low point defect concentration near GB

[1] F. Soisson and T. Jourdan, Acta Materialia 103 (2016) 870—881
[2] E. Martinez, et al., Physical Review Letters 120 (2018) 106101

Conclusions

AM microstructures representative of 316 SS

- Parameterized using experimental + atomistic data + parameter tuning
- Dislocation density-based sink was employed for static cell walls
- In comparing RIS at dislocation cell walls and HAGB, simulations predict lower peak concentrations

Microstructure evolution in ferritic FeCr alloy

- RIS model predicts cross-over of Cr from depletion at high T to enrichment at low T
- Spatially-resolved simulations demonstrate RIS and α' precipitation simultaneously
- Current limitation: dilute Cr concentration in the calculation of Onsager transport coefficients